01

Dynamics of entanglement of an isolated atom and two Jaynes–Cummings atoms

© A.R. Bagrov, E.K. Bashkirov

Samara National Research University,
443086 Samara, Russia
e-mail: bashkirov.ek@ssau.ru

Received November 30, 2024
Revised November 30, 2024
Accepted November 30, 2024

The exact solution of a model consisting of three identical two-level atoms (qubits), one of which is in a free state and the other two are trapped in individual lossless single-mode resonators and interact resonantly with the selected mode of their resonator, is found. Based on the exact solution, the pairwise negativities and the fidelities for the two initial genuine entangled W-type qubit states and the genuine entangled GHZ-type qubit state, as well as the thermal states of the resonator fields, are calculated. The influence of thermal noise intensities of resonators and initial states of qubits on the amount of their entanglement in the process of further evolution, as well as on the features of the qubits entanglement sudden death phenomenon is investigated.

Keywords: qubits, genuine entangled W-type states and GHZ-states, thermal fields, entanglement, pairwise negativity, fidelity, sudden death of entanglement.

DOI: 10.61011/TP.2025.05.61116.433-24

Introduction

The quantum entangled states are a fundamental resource in quantum processing of information, in particular, in physics of quantum computing and quantum communications [1,2]. Cavity quantum electrodynamics (CQED) which studies the interaction of qubit systems with quantum fields of resonators under conditions that can be most easily implemented experimentally, is a priority tool for studying the properties of entangled states of multi-qubit systems [3,4]. In recent years, it has become possible to use CQED to experimentally observe entangled states of qubits of various physical natures, such as neutral atoms, ions in magnetic traps, superconducting rings with Josephson junctions, quantum dots, and impurity spins [5–10]. The theoretical studies of the qubit systems interacting with the highlighted resonators modes within CQED are based on Jaynes–Cummings model (JCM) and its generalizations and expansions (see references in [11]). JCM is the simplest fully quantum exact solvable physical model that describes the interaction of a natural or artificial two-level atom (qubit) with a lossless single-mode resonator field. In recent years, JCM has been used to describe a wide range of quantum effects of the interaction of a single atom with a quantum electromagnetic field. To study a wider range of quantum phenomena caused by the interaction of qubits with the resonators quantum fields, numerous generalizations and extensions of JCM have been considered in recent years, in particular, various versions of polyatomic JCM. The use of entangled states for quantum computing and communications suggests the need to choose appropriate criteria to quantify the degree of the qubit entanglement [12]. Although the general properties of entangled states have been studied in sufficient detail, the quantitative criteria for qubit entanglement have so far been introduced only for the two-qubit systems [13–15]. In case of the multi-qubit systems, similar criteria have not been introduced to date. The non-zero values of the entanglement criteria used, introduced for the multi-qubit systems, indicate only the presence of entanglement in the system, but do not allow for a rigorous quantitative assessment of the degree of qubits entanglement [16]. The difficulties in theoretical description of entangled states rise significantly with the growing number of qubits in the system. Therefore, at present, special attention is paid to the study of the dynamics of entanglement of the three-qubit systems. Attention to such systems is also attracted due to the possibility of using three-qubit models in theoretical analysis of the universal quantum gates' behavior in manipulating the three-qubit quantum entangled states [17–19]. To perform arbitrary calculations, a set of universal gates shall be deployed in the quantum computer. Such set may include, for example, the two-qubit gates, e.g., controlled-„NOT“ (CNOT) [17], and single-qubit rotations. Alternatively, three-qubit gates such as Toffoli or Fredkin gates may be used [18,19]. Three-qubit gates are also important in applications such as quantum error correction [20]. Three-qubit quantum entangled states have been experimentally implemented in a series of tests in systems of superconducting qubits, trapped ions, and impurity spins [21–27].

Recently, many theoretical studies have been carried out on the behavior pattern of various versions of triatomic JCMs. The authors of papers [28–35] considered a three-particle model consisting of three identical two-level atoms, each of which is locked in an individual single-mode resonator. In this case, each atom resonantly interacts with

the field of its eigen resonator via single-photon processes. The authors examined the behavior pattern of such a ternary JCM for various initial correlated states of qubits and resonator fields. Another version of the triatomic JCM was reviewed in [36–44]. The authors of these papers examined the pattern of entanglement of three identical two-level atoms interacting with a dedicated mode of the common quantized resonator field for the Fock, coherent, and thermal states of the resonator field, as well as for separable, bi-separable, and genuine entangled atomic states. Finally, in papers [45–48], a three-qubit system consisting of an isolated atom and two atoms trapped in a single-mode optical resonator was considered. The authors investigated the dynamics of entanglement of atoms for various initial states of resonator field and entangled states of atoms.

In this paper, we investigated the exact behavior pattern of entanglement of three identical three-level atoms in a new three-atom model consisting of an isolated atom and two atoms, each of which is trapped in an individual optical or microwave resonator and resonantly interacts with the single-mode field of this individual resonator via single-photon transitions. We have found an exact expression for the evolution operator of the considered triatomic model. Based on the exact solution, we investigated the behavior pattern of the reviewed model for the initial entangled W- and GHZ-states of atoms, and thermal states as the initial states of the resonator fields. The criterion of atomic entanglement in case of initial W states were pairwise negativity and fidelity, and in case of GHZ states — fidelity. The choice of thermal states of the resonator fields was determined by the following circumstance. Electromagnetic fields of resonators are used to control the states of natural and artificial atoms (qubits), while thermal photons are always present in resonators. The temperatures of resonators vary from nK for trapped magnetic ions to room temperatures for the nitrogen-substituted vacancies in diamond, which means a wide range of the intensities of thermal fields of such resonators. Due to the interaction of atoms with thermal fields of the resonators, oscillations of Rabi parameter of atoms entanglement are possible, as well as the sudden death of atoms entanglement, i.e., the disappearance of entanglement at times shorter than the decoherence time. The presence of Rabi oscillations and destruction of the initial entanglement can lead to errors in qubits states readout. Therefore, the study of behavior pattern of thermal entanglement of atoms in triatomic models is of undoubted interest for quantum computer science.

1. Model and its exact solution

Let's describe the model of interest. Let's consider three identical two-level atoms (qubits) A, B and C. The qubit A moves freely outside the resonators, while the other two qubits B, C are located in two independent resonators and each resonantly interacts with the single-mode quantized field of its ideal resonator. The Hamiltonian of such a system in the dipole approximation and the rotating wave approximation will be written as

$$\hat{H}_{int} = \hbar\gamma\left(\hat{\sigma}_B^+\hat{b} + \hat{\sigma}_B^-\hat{b}^+\right) + \hbar\gamma\left(\hat{\sigma}_C^+\hat{c} + \hat{\sigma}_C^-\hat{c}^+\right), \quad (1)$$

where $\hat{\sigma}_i^+ = |+\rangle_{ii}\langle -|$ and $\hat{\sigma}_i^- = |-\rangle_{ii}\langle +|$ — are raising and lowering operators in i-th qubit, $\hat{b}(\hat{c})$ and $\hat{b}^+(\hat{c}^+)$ are operators of the destruction and creation of photons $n_B(n_C)$ in the resonator mode. When writing the Hamiltonian (1) we assumed that the constants of B and C qubits interaction with resonators are equal $\gamma_C = \gamma_B = \gamma$.

To find the state vector of the model described by the Hamiltonian (1), at subsequent moments of time t it is convenient to classify all the initial states of the system by introducing a new parameter $N = N_B + N_C$. Here

$$N_B(n_B, n_{q_B}) = \begin{cases} 0, & \text{if } n_{q_B} = n_B = 0, \\ 1, & \text{if } n_{q_B}=0,\ n_B \geq 1 \text{ or } n_{q_B}=1,\ n_B \geq 0, \end{cases}$$

$$N_C(n_C, n_{q_C}) = \begin{cases} 0, & \text{if } n_{q_C} = n_C = 0, \\ 1, & \text{if } n_{q_C}=0,\ n_C \geq 1 \text{ or } n_{q_C}=1,\ n_C \geq 0, \end{cases}$$

where n_{q_B} and n_{q_C} — number of excited qubits in resonators B and C respectively, n_B and n_C — number of photons in the mode of resonators B and C, respectively. Therefore, parameter N may have only the following values: 0, 1 and 2.

For $N = 2$ the evolution of the state vector will take place in a 4-dimensional Hilbert space. There are two sets of basis vectors. The distance between them are caused by the state of atom A. For an excited atom A, the basis vectors can be written as:

$$|+_A, +_B, +_C, n_B, n_C\rangle,\ |+_A, +_B, -_C, n_B, n_C + 1\rangle,$$
$$|+_A, -_B, +_C, n_B + 1, n_C\rangle,\ |+_A, -_B, -_C, n_B + 1, n_C + 1\rangle, \quad (2)$$

and for the ground state of atom A it will be more convenient to write the basis vectors as follows:

$$|-_A, +_B, +_C, n_B, n_C\rangle,\ |-_A, +_B, -_C, n_B, n_C + 1\rangle,$$
$$|-_A, -_B, +_C, n_B + 1, n_C\rangle,\ |-_A, -_B, -_C, n_B + 1, n_C + 1\rangle. \quad (3)$$

If the condition $N = 1$ is fulfilled, then the evolution of the state vector of the system under consideration occurs in a 2-dimensional Hilbert space. There are four sets of basis vectors. Two sets of basic vectors arise from qubit A, and the other two sets arise from evolution of the state vector of either qubit B or qubit C. It is convenient further to represent these sets in the form:

$$|+_A, +_B, -_C, n_B, 0\rangle, \quad |+_A, -_B, -_C, n_B + 1, 0\rangle;$$
$$|+_A, -_B, +_C, 0, n_C\rangle, \quad |+_A, -_B, -_C, 0, n_C + 1\rangle, \quad (4)$$
$$|-_A, +_B, -_C, n_B, 0\rangle, \quad |-_A, -_B, -_C, n_B + 1, 0\rangle;$$
$$|-_A, -_B, +_C, 0, n_C\rangle, \quad |-_A, -_B, -_C, 0, n_C + 1\rangle. \quad (5)$$

In case of $N = 0$ there's no any evolution of vectors. The existing two basic sets:

$$|+_A, -_B, -_C, 0, 0\rangle, \tag{6}$$

$$|-_A, -_B, -_C, 0, 0\rangle. \tag{7}$$

For the case $N = 2$ we've found the evolution operator $\hat{U}$ in the basis (2), (3):

$$\hat{U} = \begin{pmatrix} U_{11} & U_{12} & U_{13} & 0 & U_{15} & 0 & 0 & 0 \\ U_{21} & U_{22} & U_{23} & 0 & U_{25} & 0 & 0 & 0 \\ U_{31} & U_{32} & U_{33} & 0 & U_{35} & 0 & 0 & 0 \\ 0 & 0 & 0 & U_{44} & 0 & U_{46} & U_{47} & U_{48} \\ U_{51} & U_{52} & U_{53} & 0 & U_{55} & 0 & 0 & 0 \\ 0 & 0 & 0 & U_{64} & 0 & U_{66} & U_{67} & U_{68} \\ 0 & 0 & 0 & U_{74} & 0 & U_{76} & U_{77} & U_{78} \\ 0 & 0 & 0 & U_{84} & 0 & U_{86} & U_{87} & U_{88} \end{pmatrix},$$

$$\begin{pmatrix} |+_A, +_B, +_C, n_B, n_C\rangle \\ |+_A, +_B, -_C, n_B, n_C + 1\rangle \\ |+_A, -_B, +_C, n_B + 1, n_C\rangle \\ |-_A, +_B, +_C, n_B, n_C\rangle \\ |+_A, -_B, -_C, n_B + 1, n_C + 1\rangle \\ |-_A, +_B, -_C, n_B, n_C + 1\rangle \\ |-_A, -_B, +_C, n_B + 1, n_C\rangle \\ |-_A, -_B, -_C, n_B + 1, n_C + 1\rangle \end{pmatrix} \leftrightarrow \begin{pmatrix} 1 \\ 2 \\ 3 \\ 4 \\ 5 \\ 6 \\ 7 \\ 8 \end{pmatrix}, \tag{8}$$

where the elements of the evolution operator $U_{ij} \equiv U_{ij}(n_B, n_C, t)$ are written as follows:

$$U_{11} = \begin{cases} \cos^2\left[\gamma t\sqrt{n_B + 1}\right], & \text{if } n_B = n_C, \\ \frac{1}{2}\Big[\cos(t\theta_1) + \cos(t\theta_2)\Big], & \text{in other cases,} \end{cases}$$

$$U_{21} = \begin{cases} -i\cos\left[\gamma t\sqrt{n_B + 1}\right]\sin\left[\gamma t\sqrt{n_C + 1}\right], & \text{if } n_B = n_C, \\ -\frac{i\left[\sqrt{(n_B+1)}(\sin(t\theta_2)\theta_1 - \sin(t\theta_1)\theta_2) + \sqrt{(n_C+1)}(\sin(t\theta_2)\theta_1 + \sin(t\theta_1)\theta_2)\right]}{2\gamma\sqrt{(n_C - n_B)^2}}, & \\ & \text{in other cases,} \end{cases}$$

$$U_{31} = \begin{cases} -i\cos\left[\gamma t\sqrt{n_C + 1}\right]\sin\left[\gamma t\sqrt{n_B + 1}\right], & \text{if } n_B = n_C, \\ -\frac{i\left[\sqrt{(n_C+1)}(\sin(t\theta_2)\theta_1 - \sin(t\theta_1)\theta_2) + \sqrt{(n_B+1)}(\sin(t\theta_2)\theta_1 + \sin(t\theta_1)\theta_2)\right]}{2\gamma\sqrt{(n_C - n_B)^2}}, & \\ & \text{in other cases,} \end{cases}$$

$$U_{51} = \begin{cases} -\sin^2\left[\gamma t\sqrt{n_B + 1}\right], & \text{if } n_B = n_C, \\ \frac{1}{2}\Big[\cos(t\theta_2) - \cos(t\theta_1)\Big], & \text{in other cases,} \end{cases}$$

$$U_{11} = U_{22} = U_{33} = U_{44} = U_{55} = U_{66} = U_{77} = U_{88},$$

$$U_{21} = U_{12} = U_{53} = U_{35} = U_{64} = U_{46} = U_{87} = U_{78},$$

$$U_{31} = U_{13} = U_{52} = U_{25} = U_{74} = U_{47} = U_{86} = U_{68},$$

$$U_{51} = U_{15} = U_{32} = U_{23} = U_{84} = U_{48} = U_{76} = U_{67},$$

where

$$\theta_1 = \gamma\sqrt{\left(\sqrt{n_C + 1} - \sqrt{n_B + 1}\right)^2},$$

$$\theta_2 = \gamma\sqrt{\left(\sqrt{n_C + 1} + \sqrt{n_B + 1}\right)^2}.$$

For the case $N = 1$ we've found the evolution operator $\hat{S}$ in the basis (4), (5):

$$\hat{S} = \begin{pmatrix} S_{11} & S_{12} & 0 & 0 & 0 & 0 & 0 & 0 \\ S_{21} & S_{22} & 0 & 0 & 0 & 0 & 0 & 0 \\ 0 & 0 & S_{33} & S_{34} & 0 & 0 & 0 & 0 \\ 0 & 0 & S_{43} & S_{44} & 0 & 0 & 0 & 0 \\ 0 & 0 & 0 & 0 & S_{55} & S_{56} & 0 & 0 \\ 0 & 0 & 0 & 0 & S_{65} & S_{66} & 0 & 0 \\ 0 & 0 & 0 & 0 & 0 & 0 & S_{77} & S_{78} \\ 0 & 0 & 0 & 0 & 0 & 0 & S_{87} & S_{88} \end{pmatrix},$$

$$\begin{pmatrix} |+_A, +_B, -_C, n_B, 0\rangle \\ |+_A, -_B, -_C, n_B + 1, 0\rangle \\ |+_A, -_B, +_C, 0, n_C\rangle \\ |+_A, -_B, -_C, 0, n_C + 1\rangle \\ |-_A, +_B, -_C, n_B, 0\rangle \\ |-_A, -_B, -_C, n_B + 1, 0\rangle \\ |-_A, -_B, +_C, 0, n_C\rangle \\ |-_A, -_B, -_C, 0, n_C + 1\rangle \end{pmatrix} \longleftrightarrow \begin{pmatrix} 1 \\ 2 \\ 3 \\ 4 \\ 5 \\ 6 \\ 7 \\ 8 \end{pmatrix}, \tag{9}$$

where the elements of the evolution operator $\hat{S}$ are written as follows:

$$S_{11}(n_B, t) = S_{22}(n_B, t) = S_{55}(n_B, t) = S_{66}(n_B, t) = \cos(\gamma t\sqrt{n_B + 1}),$$

$$S_{21}(n_B, t) = S_{12}(n_B, t) = S_{65}(n_B, t) = S_{56}(n_B, t) = -i\sin(\gamma t\sqrt{n_B + 1}),$$

$$S_{33}(n_C, t) = S_{44}(n_C, t) = S_{77}(n_C, t) = S_{88}(n_C, t) = \cos(\gamma t\sqrt{n_C + 1}),$$

$$S_{43}(n_C, t) = S_{34}(n_C, t) = S_{87}(n_C, t) = S_{78}(n_C, t) = -i\sin(\gamma t\sqrt{n_C + 1}).$$

As the initial states of the qubit subsystem we've selected W-type states:

$$|W_1(0)\rangle_{ABC} = \cos\theta|+_A, +_B, -_C\rangle + \sin\theta\sin\varphi|+_A, -_B, +_C\rangle + \sin\theta\cos\varphi|-_A, +_B, +_C\rangle, \tag{10}$$

$$|W_2(0)\rangle_{ABC} = \cos\theta|-_A, -_B, +_C\rangle + \sin\theta\sin\varphi|-_A, +_B, -_C\rangle + \sin\theta\cos\varphi|+_A, -_B, -_C\rangle, \tag{11}$$

or GHZ-type states:

$$|G_1(0)\rangle_{ABC} = \cos\phi|+_A, +_B, +_C\rangle + \sin\phi|-_A, -_B, -_C\rangle. \tag{12}$$

Here θ, φ, ϕ — parameters defining the initial degree of entanglement of qubits A, B and C. As the initial state of the resonant cavity field, we choose a single-mode thermal field, the density matrix of which is expressed by the formula:

$$\Xi_{F_{n_B}}(0) = \sum_{n_B} p_{n_B} |n_B\rangle\langle n_B|, \quad \Xi_{F_{n_C}}(0) = \sum_{n_C} p_{n_C} |n_C\rangle\langle n_C|. \tag{13}$$

Here, the statistical weights p_{n_B} and p_{n_C} are expressed by the formula:

$$p_{n_B} = \frac{\bar{n}_B^{n_B}}{(\bar{n}_B + 1)^{n_B+1}}, \quad p_{n_C} = \frac{\bar{n}_C^{n_C}}{(\bar{n}_C + 1)^{n_C+1}},$$

where $\bar{n}_B$ and $\bar{n}_C$ — average number of thermal photons in resonators B and C respectively, which is determined by the standard Bose–Einstein formula:

$$\bar{n}_{B(C)} = (\exp[\hbar\omega/k_{\mathrm{B}} T_{B(C)}] - 1)^{-1}.$$

Here k_{B} — Boltzmann constant, $T_{B(C)}$ — temperature of resonator $B(C)$.

Now, thanks to evolution operators (8) and (9) it is possible to find the wave function at the moment of time t for any initial state of the qubits for the Fock state of the resonator fields using the equation $|\psi_{n_B n_C}(t)\rangle = \hat{U}|\psi(0)\rangle_{ABC}|n_B\rangle|n_C\rangle$, where $|\psi_{n_B n_C}(t)\rangle$ — wave function describing the state of the system, which includes qubits and the resonant field mode, at an arbitrary moment of time t.

To calculate any known entanglement criteria for three-qubit systems, we need to calculate the reduced two- and three-qubit density matrices of the complete system. As a first step to realize this goal, it is required to calculate the density matrix of the complete system „three qubits + mode of B resonator field + mode of C“ resonator field. Knowing the explicit form of the time wave functions $|\psi_{n_B n_C}(t)\rangle$ we can construct the density matrix of the complete system

$$\Xi_{ABCF_{n_B}F_{n_C}} = \sum_{n_B=0}^{\infty}\sum_{n_C=0}^{\infty} p_{n_B} p_{n_C} |\psi_{n_B n_C}(t)\rangle\langle\psi_{n_B n_C}(t)|. \tag{14}$$

For states (10)–(12) the formula (14) is written as follows:

$$\begin{aligned}\Xi_{ABCF_{n_B}F_{n_C}} &= \sum_{n_B=0}^{\infty}\sum_{n_C=0}^{\infty} p_{n_B} p_{n_C} |\psi_{n_B n_C}(t)\rangle\langle\psi_{n_B n_C}(t)| \\ &= p_{0_B} p_{0_C} |\psi_{0_B 0_C}(t)\rangle\langle\psi_{0_B 0_C}(t)| + \sum_{n_C=1}^{\infty} p_{n_C} p_{0_B} |\psi_{0_B n_C}(t)\rangle \\ &\times \langle\psi_{0_B n_C}(t)| + \sum_{n_B=1}^{\infty} p_{n_B} p_{0_C} |\psi_{n_B 0_C}(t)\rangle\langle\psi_{n_B 0_C}(t)| \\ &+ \sum_{n_C=1}^{\infty} p_{n_C} \sum_{n_B=1}^{\infty} p_{n_B} |\psi_{n_B n_C(t)}\rangle\langle\psi_{n_B n_C}(t)|.\end{aligned}$$

To get the three-qubit density matrix Ξ_{ABC}, it is enough to take the trace based on the variables of the field of B resonator and C resonator:

$$\Xi_{ABC}(t) = Tr_{F_{n_B}} Tr_{n_C} \Xi_{ABCF_{n_B}F_{n_C}}. \tag{15}$$

To compute the two-qubit density matrix it is required to average the three-qubit density matrix (15) over the variables of the third qubit i.e.

$$\Xi_{ij}(t) = Tr_k \rho_{ABC}(t)(i, j, k = A, B, C; i \neq j, j \neq k, i \neq k). \tag{16}$$

2. Computation of the negativity criterion and fidelity

When studying the entanglement of qubits in the considered model for the genuine entangled W-type states, we will use the criterion of negativity of pairs of qubits as a quantitative criterion of entanglement. We need to define the negativity for qubits i and j in traditional way [13–15]:

$$\varepsilon_{ij} = -2\sum_k (\lambda_{ij})_k^-, \tag{17}$$

where λ_{ij} — negative eigen values of the reduced two-qubit density matrix $\Xi_{ij}^T(t)$ partially transposed over the variables of one qubit, which has the following form for W-states (10),(11):

$$\Xi_{ij}^T(t) = \begin{pmatrix} \Xi_{11}^{ij} & 0 & 0 & \Xi_{32}^{ij} \\ 0 & \Xi_{22}^{ij} & 0 & 0 \\ 0 & 0 & \Xi_{33}^{ij} & 0 \\ \Xi_{23}^{ij} & 0 & 0 & \Xi_{44}^{ij} \end{pmatrix}, \begin{pmatrix} |+_i, +_j\rangle \\ |+_i, -_j\rangle \\ |-_i, +_j\rangle \\ |-_i, -_j\rangle \end{pmatrix} \longleftrightarrow \begin{pmatrix} 1 \\ 2 \\ 3 \\ 4 \end{pmatrix}. \tag{18}$$

Then the formula for the negativity criterion (17) is written as:

$$\varepsilon_{ij} = \sqrt{(\Xi_{44}^{ij} - \Xi_{11}^{ij})^2 + 4|\Xi_{23}^{ij}|^2} - \Xi_{11}^{ij} - \Xi_{44}^{ij}. \tag{19}$$

Let's write down the elements of the two-qubit density matrix (18) Ξ_{AB}, which are used in formula (19) to calculate negativity, for the state (10):

$$\begin{aligned}\Xi_{11}^{AB} &= \sum_{n_C=1}^{\infty} p_{n_C} \sum_{n_B=1}^{\infty} p_{n_B} \Big[\cos^2\theta \big(|U_{12}(n_B, n_C - 1, t)|^2 \\ &+ |U_{22}(n_B, n_C - 1, t)|^2\big) + \sin^2\theta \sin^2\varphi \big(|U_{13}(n_B - 1, n_C, t)|^2 \\ &+ |U_{23}(n_B - 1, n_C, t)|^2\big)\Big] + \cos^2\theta p_{0_B} \\ &\times \sum_{n_C=1}^{\infty} p_{n_C} \Big[|U_{12}(0, n_C - 1, t)|^2 + |U_{22}(0, n_C - 1, t)|^2\Big] \\ &+ p_{0_C} \sum_{n_B=1}^{\infty} p_{n_B} \Big[\cos^2\theta |S_{11}(n_B, t)|^2 + \sin^2\theta \sin^2 \\ &\times \varphi \left(|U_{13}(n_B - 1, 0, t)|^2 + |U_{23}(n_B - 1, 0, t)|^2\right)\Big] \\ &+ p_{0_B} p_{0_C} \cos^2\theta |S_{11}(0, t)|^2,\end{aligned}$$

$$\Xi_{23}^{AB} = \sin^2\theta \sin\varphi \cos\varphi \Bigg\{ \sum_{n_C=1}^{\infty} p_{n_C} \sum_{n_B=1}^{\infty} p_{n_B} \Big[U_{33}(n_B-1, n_C, t) \times U_{44}^*(n_B, n_C, t) + U_{53}(n_B-1, n_C, t) U_{64}^*(n_B, n_C, t) \Big] + p_{0_B} \times \sum_{n_C=1}^{\infty} p_{n_C} \Big[S_{33}(n_C, t) U_{44}^*(0, n_C, t) + S_{43}(n_C, t) U_{64}^*(0, n_C, t) \Big] + p_{0_C} \sum_{n_B=1}^{\infty} p_{n_B} \Big[U_{33}(n_B-1, 0, t) U_{44}^*(n_B, 0, t) + U_{53}(n_B-1, 0, t) U_{64}^*(n_B, 0, t) \Big] + p_{0_B} p_{0_C} \Big[S_{33}(0, t) \times U_{44}^*(0, 0, t) + S_{43}(0, t) U_{64}^*(0, 0, t) \Big] \Bigg\},$$

$$\Xi_{44}^{AB} = \sin^2\theta \cos^2\varphi \sum_{n_C=0}^{\infty} p_{n_C} \sum_{n_B=0}^{\infty} p_{n_B} \Big[|U_{74}(n_B, n_C, t)|^2 + |U_{84}(n_B, n_C, t)|^2 \Big].$$

The elements of the two-qubit density matrix (18) Ξ_{BC}, which are used in formula (19) to calculate negativity, for the state (10):

$$\Xi_{11}^{BC} = \sum_{n_B=1}^{\infty} p_{n_B} \sum_{n_C=1}^{\infty} p_{n_C} \Big[\cos^2\theta |U_{12}(n_B, n_C-1, t)|^2 + \sin^2\theta \sin^2\varphi |U_{13}(n_B-1, n_C, t)|^2 + \sin^2\theta \cos^2 \times \varphi |U_{44}(n_B, n_C, t)|^2 \Big] + p_{0_B} \sum_{n_C=1}^{\infty} p_{n_C} \Big[\cos^2\theta |U_{12}(0, n_C-1, t)|^2 + \sin^2\theta \cos^2\varphi |U_{44}(0, n_C, t)|^2 \Big] + p_{0_C} \sum_{n_B=1}^{\infty} p_{n_B} \Big[\sin^2\theta \sin^2 \times \varphi |U_{13}(n_B-1, 0, t)|^2 + \sin^2\theta \cos^2\varphi |U_{44}(n_B, 0, t)|^2 \Big] + \sin^2\theta \cos^2\varphi p_{0_B} p_{0_C} |U_{44}(0, 0, t)|^2,$$

$$\Xi_{23}^{BC} = \sin\theta \cos\theta \sin\varphi \Bigg\{ \sum_{n_C=1}^{\infty} p_{n_C} \sum_{n_B=1}^{\infty} p_{n_B} \Big[U_{22}(n_B, n_C-1, t) \times U_{33}^*(n_B-1, n_C, t) \Big] + \sin\theta p_{0_B} \sum_{n_C=1}^{\infty} p_{n_C} \Big[U_{22}(0, n_C-1, t) \times S_{33}^*(n_C, t) \Big] + p_{0_C} \sum_{n_B=1}^{\infty} p_{n_B} \Big[S_{11}(n_B, t) U_{33}^*(n_B-1, 0, t) \Big] + p_{0_B} p_{0_C} S_{11}(0, t) S_{33}^*(0, t) \Bigg\},$$

$$\Xi_{44}^{BC} = \sum_{n_C=1}^{\infty} p_{n_C} \sum_{n_B=1}^{\infty} p_{n_B} \Big[\cos^2\theta |U_{52}(n_B, n_C-1, t)|^2 + \sin^2\theta \sin^2\varphi |U_{53}(n_B-1, n_C, t)|^2 + \sin^2\theta \cos^2 \times \varphi |U_{84}(n_B, n_C, t)|^2 \Big] + p_{0_B} \sum_{n_{C=1}}^{\infty} \Big[\sin^2\theta \sin^2\varphi |S_{43}(n_C, t)|^2 + \cos^2\theta |U_{52}(0, n_C-1, t)|^2 + \sin^2\theta \cos^2\varphi |U_{84}(0, n_C, t)|^2 \Big] + p_{0_C} \sum_{n_B=1}^{\infty} p_{n_B} \Big[\cos^2\theta |S_{21}(n_B, t)|^2 + \sin^2\theta \sin^2 \times \varphi |U_{53}(n_B-1, 0, t)|^2 + \sin^2\theta \cos^2\varphi |U_{84}(n_B, 0, t)|^2 \Big] + p_{0_B} p_{0_C} \Big[\cos^2\theta |S_{21}(0, t)|^2 + \sin^2\theta \sin^2\varphi |S_{43}(0, t)|^2 + \sin^2\theta \cos^2\varphi |U_{84}(0, 0, t)|^2 \Big].$$

Let's write down the elements of the two-qubit density matrix (18) Ξ_{AB}, which are used in formula (19) to calculate negativity, for the state (11):

$$\Xi_{11}^{AB} = \sin^2\theta \cos^2\varphi \sum_{n_C=1}^{\infty} p_{n_C} \sum_{n_B=1}^{\infty} p_{n_B} \Big[|U_{15}(n_B-1, n_C-1, t)|^2 + |U_{25}(n_B-1, n_C-1, t)|^2 \Big] + \sin^2\theta \cos^2\varphi p_{0_C} \times \sum_{n_B=1}^{\infty} p_{n_B} |S_{12}(n_B-1, t)|^2,$$

$$\Xi_{33}^{AB} = \sum_{n_C=1}^{\infty} p_{n_C} \sum_{n_B=1}^{\infty} p_{n_B} \Big[\sin^2\theta \sin^2\varphi \Big(|U_{46}(n_B, n_C-1, t)|^2 + |U_{66}(n_B, n_C-1, t)|^2 \Big) + \cos^2\theta \Big(|U_{47}(n_B-1, n_C, t)|^2 + |U_{67}(n_B-1, n_C, t)|^2 \Big) \Big] + \sin^2\theta \sin^2\varphi p_{0_B} \sum_{n_C=1}^{\infty} p_{n_C} \times \Big[|U_{46}(0, n_C-1, t)|^2 + |U_{66}(0, n_C-1, t)|^2 \Big] + p_{0_C} \sum_{n_B=1}^{\infty} p_{n_B} \Big[\sin^2\theta \sin^2\varphi |S_{55}(n_B, t)|^2 + \cos^2\theta \Big(|U_{47}(n_B-1, 0, t)|^2 + |U_{67}(n_B-1, 0, t)|^2 \Big) \Big] + p_{0_B} p_{0_C} \sin^2\theta \sin^2\varphi |S_{55}(0, t)|^2,$$

$$\Xi_{44}^{AB} = \sum_{n_C=1}^{\infty} p_{n_C} \sum_{n_B=1}^{\infty} p_{n_B} \Big[\sin^2\theta \sin^2\varphi \Big(|U_{76}(n_B, n_C - 1, t)|^2 + |U_{86}(n_B, n_C - 1, t)|^2 \Big) + \cos^2\theta \Big(|U_{77}(n_B - 1, n_C, t)|^2 + |U_{87}(n_B - 1, n_C, t)|^2 \Big) \Big] + p_{0_B} \sum_{n_C=1}^{\infty} p_{n_C} \Big[\cos^2\theta \Big(|S_{77}(n_C, t)|^2 + |S_{87}(n_C, t)|^2 \Big) + \sin^2\theta \sin^2\varphi \Big(|U_{76}(0, n_C - 1, t)|^2 + |U_{86}(0, n_C - 1, t)|^2 \Big) \Big] + p_{0_C} \sum_{n_B=1}^{\infty} p_{n_B} \Big[\sin^2\theta \sin^2\varphi |S_{65}(n_B, t)|^2 + \cos^2\theta \Big(|U_{77}(n_B - 1, 0, t)|^2 + |U_{87}(n_B - 1, 0, t)|^2 \Big) \Big] + p_{0_B} p_{0_C} \Big[\sin^2\theta \sin^2\varphi |S_{65}(0, t)|^2 + \cos^2\theta \Big(|S_{77}(0, t)|^2 + |S_{87}(0, t)|^2 \Big) \Big].$$

The elements of the two-qubit density matrix (18) Ξ_{BC}, which are used in formula (19) to calculate negativity, for the state (11):

$$\Xi_{11} = \sum_{n_C=1}^{\infty} p_{n_C} \sum_{n_B=1}^{\infty} p_{n_B} \Big[\sin^2\theta \cos^2\varphi |U_{15}(n_B - 1, n_C - 1, t)|^2 + \sin^2\theta \sin^2\varphi |U_{46}(n_B, n_C - 1, t)|^2 + \cos^2\theta \times |U_{47}(n_B - 1, n_C, t)|^2 \Big] + \sin^2\theta \sin^2\varphi p_{0_B} \times \sum_{n_C=1}^{\infty} p_{n_C} \Big[|U_{46}(0, n_C - 1, t)|^2 \Big] + \cos^2\theta p_{0_C} \times \sum_{n_B=1}^{\infty} p_{n_B} \Big[|U_{47}(n_B - 1, 0, t)|^2 \Big],$$

$$\Xi_{23} = \sin\theta \cos\theta \sin\varphi \Big\{ \sum_{n_C=1}^{\infty} p_{n_C} \sum_{n_B=1}^{\infty} p_{n_B} \Big[U_{66}(n_B, n_C - 1, t) \times U_{77}^*(n_B - 1, n_C, t) \Big] + p_{0_B} \sum_{n_C=1}^{\infty} p_{n_C} \Big[U_{66}(0, n_C - 1, t) \times S_{77}^*(n_C, t) \Big] + p_{0_C} \sum_{n_B=1}^{\infty} p_{n_B} \Big[S_{55}(n_B, t) U_{77}^*(n_B - 1, 0, t) \Big] + p_{0_B} p_{0_C} S_{55}(0, t) S_{77}^*(0, t) \Big\},$$

$$\Xi_{44} = \sum_{n_C=1}^{\infty} p_{n_C} \sum_{n_B=1}^{\infty} p_{n_B} \Big[\sin^2\theta \cos^2\varphi |U_{55}(n_B - 1, n_C - 1, t)|^2 + \sin^2\theta \sin^2\varphi |U_{86}(n_B, n_C - 1, t)|^2 + \cos^2\theta \times |U_{87}(n_B - 1, n_C, t)|^2 \Big] + p_{0_B} \sum_{n_C=1}^{\infty} p_{n_C} \Big[\cos^2\theta |S_{87}(n_C, t)|^2 + \sin^2\theta \cos^2\varphi |S_{44}(n_C - 1, t)|^2 + \sin^2\theta \sin^2 \times \varphi |U_{86}(0, n_C - 1, t)|^2 \Big] + p_{0_C} \sum_{n_B=1}^{\infty} p_{n_B} \Big[\sin^2\theta \cos^2\varphi \times |S_{22}(n_B - 1, t)|^2 + \sin^2\theta \sin^2\varphi |S_{65}(n_B, t)|^2 + \cos^2\theta |U_{87}(n_B - 1, 0, t)|^2 \Big] + p_{0_B} p_{0_C} \Big[\cos^2\theta |S_{87}(0, t)|^2 + \sin^2\theta \sin^2\varphi |S_{65}(0, t)|^2 + \sin^2\theta \cos^2\varphi \Big].$$

In case of GHZ states, the negativity criterion is not quite formative, since after averaging the three-qubit density matrix $\Xi_{ABC}(t)$ over the variables of one of the qubits, the two remaining qubits turn out to be non-entangled. Therefore, in this paper, as a quantitative criterion for the entanglement of qubits, we use the fidelity level of the qubits current state at the moment of time t and their initial GHZ-state. In case of the resonator thermal field, the state of the qubits at any given time is mixed. The quantitative measure of fidelity for mixed states of qubits is determined by the following formula [49]:

$$F(\Xi, \Xi') = \left(tr \sqrt{\Xi^{1/2} \Xi' \Xi^{1/2}} \right)^2. \tag{20}$$

Here Ξ — initial density matrix of the system and Ξ' — qubits density matrix in the following moments of time $t > 0$. The expression (20) is greatly simplified if we assume that at the initial moment of time the system is in clear state($\Xi = |\psi\rangle\langle\psi|$):

$$F(\Xi, \Xi') = \left(tr \sqrt{|\psi\rangle\langle\psi|\Xi'|\psi\rangle\langle\psi|} \right)^2 = \langle\psi|\Xi'|\psi\rangle = tr(\Xi\Xi'). \tag{21}$$

For GHZ-state (12) the density matrix $\Xi'_{ABC}(t)$ in the following moments of time has the following form:

$$\Xi'_{ABC}(t) = \begin{pmatrix} \Xi_{11} & 0 & 0 & 0 & 0 & 0 & 0 & \Xi_{18} \\ 0 & \Xi_{22} & 0 & 0 & 0 & 0 & 0 & 0 \\ 0 & 0 & \Xi_{33} & 0 & 0 & 0 & 0 & 0 \\ 0 & 0 & 0 & \Xi_{44} & 0 & 0 & 0 & 0 \\ 0 & 0 & 0 & 0 & \Xi_{55} & 0 & 0 & 0 \\ 0 & 0 & 0 & 0 & 0 & \Xi_{66} & 0 & 0 \\ 0 & 0 & 0 & 0 & 0 & 0 & \Xi_{77} & 0 \\ \Xi_{81} & 0 & 0 & 0 & 0 & 0 & 0 & \Xi_{88} \end{pmatrix}. \tag{22}$$

Then the formula (21) for GHZ-state (12) is transformed into the following expression:

$$F = \cos^2\phi\Xi_{11} + \sin^2\phi\Xi_{88} + \cos\phi\sin\phi\,(\Xi_{18} + \Xi_{81}), \tag{23}$$

where elements of the three-qubit density matrix $\Xi'_{ABC}(t)$ for initial state (12):

$$\Xi_{11} = \cos^2\phi\sum_{n_C=0}^{\infty} p_{n_C}\sum_{n_B=0}^{\infty} p_{n_B}\Big[|U_{11}(n_B, n_C, t)|^2\Big],$$

$$\Xi_{18} = \cos\phi\sin\phi\Bigg\{\sum_{n_C=1}^{\infty} p_{n_C}\sum_{n_B=1}^{\infty} p_{n_B}\Big[U_{11}(n_B, n_C, t) \times U^*_{88}(n_B-1, n_C-1, t)\Big] + p_{0_B}\sum_{n_C=1}^{\infty} p_{n_C}\Big[U_{11}(0, n_C, t) \times S^*_{88}(n_C-1, t)\Big] + p_{0_C}\sum_{n_B=1}^{\infty} p_{n_B}\Big[U_{11}(n_B, 0, t)S^*_{66}(n_B-1, t)\Big] + p_{0_B}p_{0_C}U_{11}(0, 0, t)\Bigg\},$$

$$\Xi_{88} = \sin^2\phi\Bigg\{\sum_{n_C=1}^{\infty} p_{n_C}\sum_{n_B=1}^{\infty} p_{n_B}\Big[|U_{88}(n_B-1, n_C-1, t)|^2\Big] + p_{0_B}\sum_{n_C=1}^{\infty} p_{n_C}\Big[|S_{88}(n_C-1, t)|^2\Big] + p_{0_C}\sum_{n_B=1}^{\infty} p_{n_B}\Big[|S_{66}(n_B-1, t)|^2\Big] + p_{0_B}p_{0_C}\Bigg\},$$

$$\Xi_{81} = \Xi^*_{18}.$$

3. Results of numerical modelling and discussion

Fig. 1, *a* shows the entanglement parameter $\varepsilon_{AB}(\gamma t)$ of the qubits A and B (or A and C) versus dimensionless time γt for the genuine entangled state of the qubits (10) from $\varphi = \pi/4$, $\theta = \arccos[1/\sqrt{3}]$ and various values of the average number of photons in the resonators modes (13). Similar dependencies for the entanglement parameter $\varepsilon_{BC}(\gamma t)$ of qubits B and C are shown in Fig. 1, *b*. In the Figures it is clearly seen both, for the qubits A and B, and for B and C that there's an effect of the entanglement sudden death and recovery in case of the resonators' thermal field. At the same time, for the qubits A and B, this effect is absent in the case of vacuum initial states of fields. For the qubits B and C the entanglement sudden death also takes place for the vacuum fields as well. From the Figures we may see that for the qubits B and C the time of entanglement recovery is significantly higher than for the qubits A and B for any strengths of the resonators' thermal fields. The Figures also show that as the average number of thermal photons increases, the maximum degree of qubit entanglement decreases rapidly. At the same time, the decrease in the maximum degree of entanglement for neighboring Rabi oscillations occurs for all pairs of qubits much faster than for the case of „three qubits in a common resonator" systems [44] or „free qubit + two qubits in the general resonator" [48]. Figure 2 shows similar dependencies for another genuine entangled initial state of qubits (11). The Figure clearly shows that the behavior of the negativity of qubits A and B (or A and C) for the considered initial state of the qubits (11) is similar to the behavior of the specified value for the initial state of qubits (10) for any thermal fields, while for qubits B and C there are significant differences in the behavior of pairwise negativity for the initial states of qubits (11) and (10) in the case of low thermal intensities of resonator fields, including vacuum states. For vacuum states of fields, the effect of sudden death of entanglement is absent, and for low field intensities, the time intervals during which entanglement is absent are significantly reduced. It should be stressed that, in contrast to the reviewed model for the earlier studied three-qubit models of „free qubit + two qubits in common resonator" or „three qubits in common resonator" the behavior of the pairwise negativities significantly differ for the initial W-states (10) and (11) for any intensities of thermal fields. For these models, the duration of time intervals between the sudden death and recovery of qubit entanglement significantly depends on the choice of W state. In addition, for the model „free qubit + two qubits in a common resonator" in the case of low intensities of the resonator's thermal field, the effect of sudden death of entanglement occurs only when the qubits are initially prepared in a state of the form (10).

It is of interest to supplement the numerical calculations of the qubit entanglement parameters for states (10) and (11) with an analysis of analytical expressions for pairwise negativities and fidelity in case of vacuum initial states of resonator fields and parameters $\varphi = \pi/4$ and $\theta = \arccos[1/\sqrt{3}]$. To complete the picture, we will also consider the calculation of fidelity $F(\gamma t)$ in this case. For the initial state (10), the pairwise negativities $\varepsilon_{AB}(\gamma t)$, $\varepsilon_{BC}(\gamma t)$ and the fidelity $F(\gamma t)$ are equal

$$\varepsilon_{AB}(\gamma t) = \frac{\sqrt{2}}{6}\Big(\sqrt{5 + 4\cos(2\gamma t) + \cos(4\gamma t)} - \sqrt{2}\Big),$$

$$\varepsilon_{BC}(\gamma t) = \frac{1}{12}\Big(2\sqrt{2}\sqrt{9 - 4\cos(2\gamma t) + 5\cos(4\gamma t)} + 4\cos(2\gamma t) - \cos(4\gamma t) - 7\Big)$$

and

$$F(\gamma t) = \frac{1}{9}\cos^2(\gamma t)\Big[2 + \cos(\gamma t)\Big]^2$$

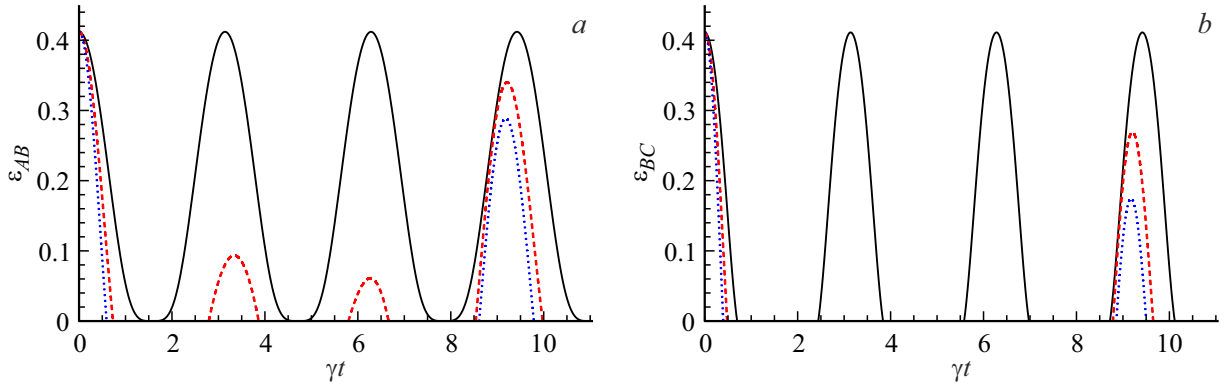

Figure 1. Negativity criterion $\varepsilon_{AB(AC)}(\gamma t)$ (a) and $\varepsilon_{BC}(\gamma t)$ (b) versus reduced time γt for the initial state of qubits (10) for $\varphi = \pi/4$, $\theta = \arccos[1/\sqrt{3}]$. In all graphs: vacuum field $n = n_B = n_C = 0$ (black solid line), $\bar{n}_B = \bar{n}_C = 0.5$ (red dashed line), $\bar{n}_B = \bar{n}_C = 1$ (blue dotted line).

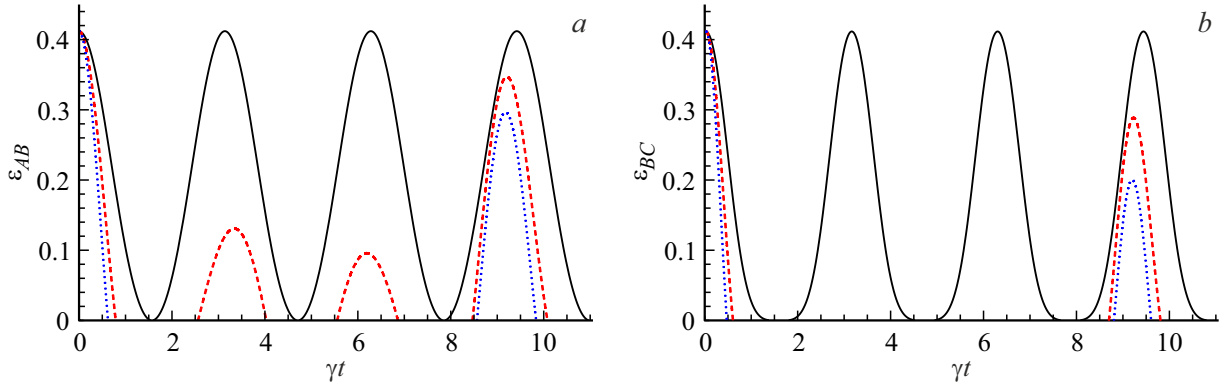

Figure 2. Negativity criterion $\varepsilon_{AB}(\gamma t)$ (a) and $\varepsilon_{BC}(\gamma t)$ (b) versus reduced time γt for the initial state of qubits (11) for $\varphi = \pi/4$, $\theta = \arccos[1/\sqrt{3}]$. In all graphs: vacuum field $n = n_B = n_C = 0$ (black solid line), $\bar{n}_B = \bar{n}_C = 0.5$ (red dashed line), $\bar{n}_B = \bar{n}_C = 1$ (blue dotted line).

respectively. For the initial state (11) the equivalent formulae are

$$\varepsilon_{AB}(\gamma t) = \frac{1}{12}\Big(\sqrt{2}\sqrt{\cos(4\gamma t) + 4\cos(2\gamma t) + 35} + 2\cos(2\gamma t) - 6\Big),$$

$$\varepsilon_{BC}(\gamma t) = \frac{1}{3}\Big(\sqrt{\cos(4\gamma t) - 2\cos(2\gamma t) + 6} + \cos(2\gamma t) - 2\Big),$$

$$F(\gamma t) = \frac{1}{9}\Big[1 + 2\cos(\gamma t)\Big]^2$$

respectively. The analysis of pairwise negativities and fidelities for states (10) and (11) shows that for the vacuum initial states of the resonator fields the maxima of the values of pairwise negatives at the moments of time $t_{k_1} = 2\pi k_1/\gamma$ $(k_1 = 1, 2, \ldots)$ correspond to the maxima of fidelity$F(\gamma t_{k_1}) = 1$. At these moments of time, the qubit system returns to its original genuine entangled W-state ((10) or (11), respectively), and resonator fields — return into vacuum states, while the maxima of pairwise negatives at the moments of time $t_{k_2} = \pi(1 + 2k_2)/\gamma$ $(k_2 = 0, 1, 2, \ldots)$ correspond to local maxima of fidelity equal to $F(\gamma t_{k_2}) = 1/9$. At the specified moments of time, the three-qubit system also occurs in the genuine entangled W-states other than the initial states, and the resonator fields return to their initial vacuum states. For the initial state (10) and (11) full wave functions of „three qubit + two modes“ system in said moments of time are

$$|\psi_{0_B 0_C}(\gamma t_{k_2})\rangle = \frac{1}{\sqrt{3}}\Big[|-_A, +_B, +_C, 0_B, 0_C\rangle - |+_A, +_B, -_C, 0_B, 0_C\rangle - |+_A, -_B, +_C, 0_B, 0_C\rangle\Big],$$

$$|\psi_{0_B 0_C}(\gamma t_{k_2})\rangle = \frac{1}{\sqrt{3}}\Big[-|-_A, -_B, +_C, 0_B, 0_C\rangle - |-_A, +_B, -_C, 0_B, 0_C\rangle + |+_A, -_B, -_C, 0_B, 0_C\rangle\Big]$$

respectively. In case of initial states of qubits (10)

$$(1/2)\arccos(3 - 2\sqrt{2}) + \pi k_3 \le \gamma t \le -(1/2) \times \arccos(3 - 2\sqrt{2}) + \pi(k_3 + 1) \ (k_3 = 0, 1, 2, \ldots),$$

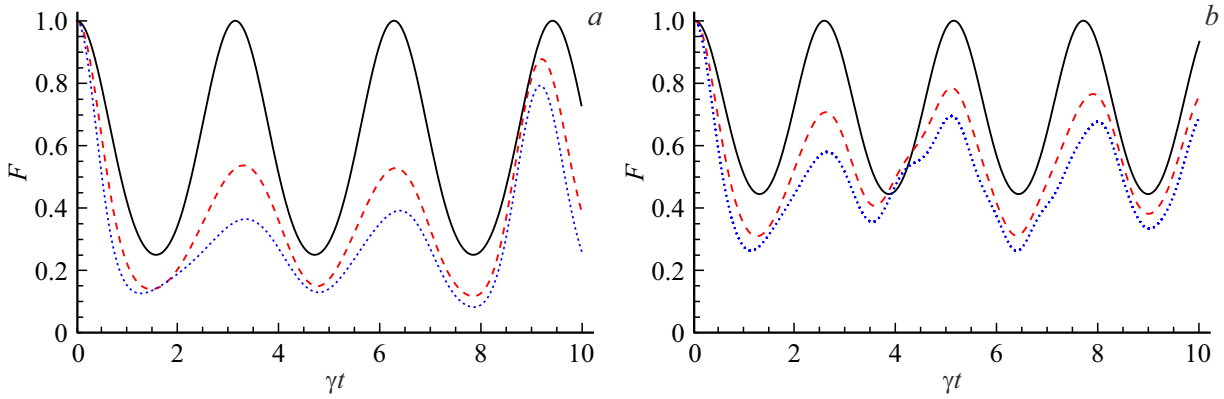

Figure 3. Fidelity $F(\gamma t)$ versus reduced time γt for the initial state of qubits (12) in case of $\phi = \pi/4$. In all graphs: vacuum field $n = n_B = n_C = 0$ (black solid line), $\bar{n}_B = \bar{n}_C = 0.5$ (red dashed line), $\bar{n}_B = \bar{n}_C = 1$ (blue dotted line). The graph (b) illustrates the plotted curve of fidelity for the model „isolated qubit + two qubits in resonator".

for the time intervals where $\varepsilon_{BC}(\gamma t) = 0$ (let's bear in mind, that when the calculated negativity is negative, its value will be taken equal to zero), the effect of sudden entanglement death takes place, the fidelity values $0 \le F(\gamma t) \le (1/9)(2-\sqrt{2})(2+\sqrt{2-\sqrt{2}})^2$ will correspond. In the specified time intervals the three qubit system, naturally, is in separable state, while complete system of „three qubits + two field modes" — in atom-field entangled state. Thus, in the moments of time $t_{k_4} = \pi(1/2 + 2k_4)/\gamma$ $(k_4 = 0, 1, 2, \ldots)$, corresponding to the minimal values of fidelity $F(\gamma t_{k_4}) = 0$, the wave function of the complete system is

$$|\psi_{0_B 0_C}(\gamma t_{k_4})\rangle = \frac{1}{\sqrt{3}}\Big[-i|+_A, -_B, -_C, 1_B, 0_C\rangle - i|+_A, -_B, -_C, 0_B, 1_C\rangle - |-_A, -_B, -_C, 1_B, 1_C\rangle\Big].$$

A reduced three-qubit density matrix corresponds to this state of the complete system.

$$\Xi_{ABC} = |-_A, -_B, -_C\rangle\langle -_A, -_B, -_C|.$$

Fig. 3, a shows the dependence of fidelity $F(\gamma t)$ on dimensionless time γt for the genuine entangled initial GHZ-state of qubits (12) for parameter $\phi = \pi/4$ and various values of the average number of photons in resonator modes. For comparison, Fig. 3, b shows the curve of fidelity $F(\gamma t)$ versus dimensionless time γt for the same initial GHZ-state and the same values of thermal field intensities, but for a model where one qubit is isolated, and the other two are locked in a common single-mode resonator. For a more complete analysis of the considered system behavior for the state (12) Figure 4 shows the behavior of the average population inversion of all three qubits for the same average number of photons as in Figure 3, a.

The analysis of temporal evolution of fidelity of the states of three qubits analytically may be carried out for the case of vacuum initial states of resonator fields. For the vacuum initial states of fields $n_B = n_C = 0$ and initial GHZ-states of qubits (12) for $\phi = \pi/4$ the fidelity is expressed as

$$F(\gamma t) = \frac{1}{16}\Big[3 + \cos(2\gamma t)\Big]^2. \qquad (24)$$

The fidelity (28) has maximal values of unity in the moments of time $t_{k_5} = \pi k_5/\gamma$ $(k_5 = 0, 1, \ldots)$. At these moments of time, for the wave function of the system, we obtain

$$|\psi_{0_B 0_C}(\gamma t_{k_5})\rangle = \frac{1}{\sqrt{2}}\Big[|+_A, +_B, +_C, 0_B, 0_C\rangle + |-_A, -_B, -_C, 0_B, 0_C\rangle\Big].$$

Thus, at specific moments of time, the system returns to its initial state.

In the moments of time $t_{k_6} = \frac{\pi}{2\gamma}\Big(1+2k_6\Big)$, where $k_6 = 0, 1, \ldots$, the fidelity has minimal values equal to 1/4. The wave function corresponding to these moments is

$$|\psi_{0_B 0_C}(\gamma t_{k_6})\rangle = \frac{1}{\sqrt{2}}\Big[|-_A, -_B, -_C, 0_B, 0_C\rangle - |+_A, -_B, -_C, 1_B, 1_C\rangle\Big]. \qquad (25)$$

The three-qubit reduced density matrix corresponding to (25) is

$$\Xi_{ABC} = \frac{1}{2}(|-_A, -_B, -_C\rangle\langle -_A, -_B, -_C| + |+_A, -_B, -_C\rangle \times \langle +_A, -_B, -_C|) = \Xi_A \otimes \Xi_B \otimes \Xi_C,$$

where

$$\Xi_A = \frac{1}{2}(|-_A\rangle\langle -_A| + |+_A\rangle\langle +_A|),$$

$$\Xi_B = |-_B\rangle\langle -_B|, \quad \Xi_C = |-_C\rangle\langle -_C|.$$

Thus, at the moments of time t_{k_6} for the initial vacuum fields of resonators, the qubits appear in a separable mixed state

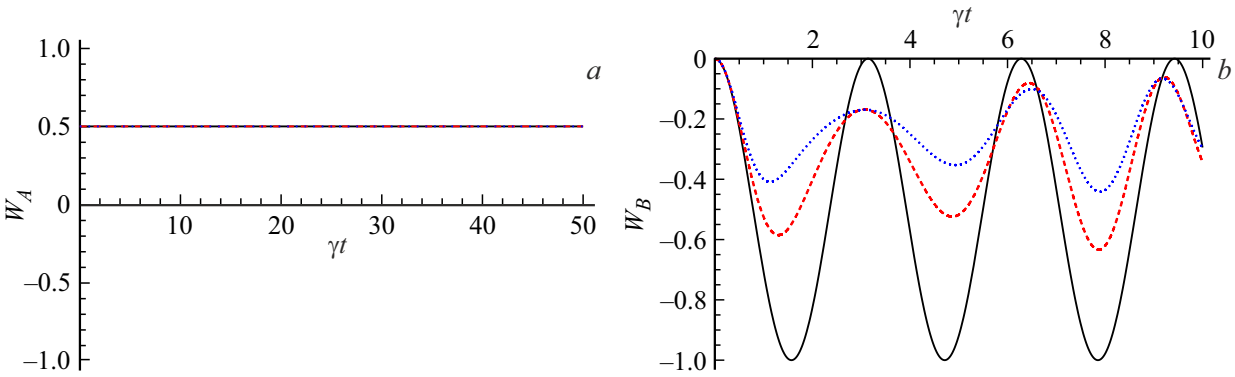

Figure 4. Inversion of population $W_A(\gamma t) + 0.5$ (a) and $W_{B(C)}(\gamma t)$ (b) versus reduced time γt for the initial state of qubits (12) for $\phi = \pi/4$. In all graphs: vacuum field $n = n_B = n_C = 0$ (black solid line), $\bar{n}_B = \bar{n}_C = 0.5$ (red dashed line), $\bar{n}_B = \bar{n}_C = 1$ (blue dotted line).

where the qubits B and C are in the ground state, and the qubit A — in the equally probable mixture of ground and excited states. Such analysis of the system evolution is fully confirmed by the behavior of the average population inversion of qubits for vacuum fields shown in Fig. 4. With higher intensity of the resonators' thermal fields, the deviation of the three-qubit state from the initial genuine entangled GHZ-state grows significantly. Additional computations of pairwise negativities $\varepsilon_{ij}(\gamma t)$ $(i, j = A, B, C,\ j \neq i)$ for a GHZ state (12) show that entanglement does not occur between the qubit pairs at any values of thermal field intensities.

Similar analysis for the model „isolated qubit + two qubits in the resonator„ (Fig. 3, b) shows that the system of qubits returns into the genuine entangled GHZ-state at the moments of time $t_{k_7} = \sqrt{2/3}\pi k_7/\gamma$ $(k_7 = 1, 2, \ldots)$. At that, maximal value of 4/9, will be reached in the moments of time $t_{k_8} = \pi\left(1 + 2k_8\right)/(\sqrt{6}\gamma)$, where $k_8 = 0, 1, \ldots$. Therefore, the initial genuine entangled GHZ-state for the reviewed model is less stable compared to the action of thermal noise than „isolated qubit + two qubits in resonator".

Conclusion

In this work, we studied the dynamics of a system of three identical two-level atoms (qubits), one of which is in a free state, and each of the rest ones is locked in an ideal resonant cavity and interacts resonantly with the electromagnetic field mode of this resonator. We have obtained an exact solution of the quantum equation for evolution operator of the considered model. On its basis we have found the exact behavior pattern of the density matrix of complete system „three qubits + two modes of field" for the initial genuinely entangled W- and GHZ-type states of the qubits and thermal fields of resonators, and also the reduced three-qubit and pairwise two-qubit density matrices have been computed. The reduced three-qubit density matrix is used to calculate the fidelity of the qubits subsystem states, and pairwise two-qubit density matrices — are used to calculate the pairwise negativity of qubits. The calculated time dependences of pairwise negativities for the two genuine entangled normalized W-states of qubits (10) and (11) and the thermal states of the resonator's electromagnetic field for different average photon numbers have shown that the resonator's thermal field does not completely destroy the initial entanglement of qubits even for relatively high intensities of thermal resonator noise, however, with the rise of average number of photons the maximum degree of qubits entanglement rapidly drops down. It is also shown that for the thermal fields of resonators, the effect of sudden death and recovery of entanglement occurs for all pairs of qubits. At the same time, for a free qubit and one of the locked qubits, this effect is absent in case of vacuum fields of resonators for both the initial state (10) and for (11). A similar behavior is typical for a pair of qubits in resonators for the initial state (11), while for the same qubits in the initial state (10), the sudden death of entanglement also occurs for the vacuum fields of resonators. As intensity of the resonators thermal fields rises, the time during which the entanglement of the qubits fades away increases significantly. The analysis of the considered system temporal behavior for vacuum states demonstrated that for initial states of qubits (10) and (11), odd maxima of pairwise negativities of qubits corresponded to the system return to the initial entangled state for the qubits and vacuum states for the fields, and even maxima — to transition of the system to states (10) and (11), but with different parameter values φ and θ.

The computations of pairwise negativities for the genuine entangled GHZ state (12) showed that entanglement was impossible between the qubit pairs at any values of thermal field intensities. The computations also showed that with higher intensity of the resonators' thermal fields, the deviation of the three-qubit state from the initial genuine entangled GHZ-state grew significantly. The analysis of temporal behavior of the considered system in case of initial state (12) and behavior of vacuum states of the fields allowed concluding that maximum values of fidelity

corresponded to the return of the qubits subsystem to the initial state (12), and return of the resonators' fields to vacuum states. A separable mixed state where locked qubits are in the ground state, and the free qubit is in an equally probable mixture of ground and excited states are characterized by minimal fidelity values. At that, the subsystem of atoms and resonators fields are in the atom-field entangled state.

Conflict of interest

The authors declare that they have no conflict of interest.

References

[1] H.-L. Huang, D. Wu, D. Fan, X. Zhu. Science China Information Sciences, **63**, 180501 (2020). DOI: 10.1007/S11432-020-2881-9

[2] N. Meher, S. Sivakumar. Eur. Phys. J. Plus., **137**, 985 (2022). DOI: 10.1140/epjp/s13360-022-03172-x

[3] S. Haroche, M. Brune, J.M. Raimond. Nature Physics, **16** (3), 243 (2020). DOI: 10.1038/s41567-020-0812-1

[4] D. De Bernardis, A. Mercurio, S. De Liberato. J. Opt. Soc. Am. B, **41** (8), C206 (2024). DOI: 10.1364/JOSAB.522786

[5] Z.-L. Xiang, S. Ashhab, J.Y. You, F. Nori. Rev. Mod. Phys., **85** (2), 623 (2013). DOI: 10.1103/RevModPhys.85.623

[6] L.M. Georgescu, S. Ashhab, F. Nori. Rev. Mod. Phys., **88** (1), 153 (2014). DOI: 10.1103/RevModPhys.86.153

[7] X. Gu, A.F. Kockum, A. Miranowicz, Y.X. Liu, F. Nori Physics Reports, **718**–**719**, 1 (2017). DOI: 10.1016/j.physrep.2017.10.002

[8] G. Wendin. Repts. Prog. Phys., **80**, 106001 (2017). DOI: 10.1088/1361-6633/aa7e1a

[9] G.-Q. Li, X.-Y. Pan. Chin. Phys., **27**, 020304 (2018). DOI: 10.1007/s11432-020-2881-9

[10] D.J. van Woerkom, P. Scarlino, J.H. Ungerer, C. Müller, J.V. Koski, A.J. Landig, C. Reichl, W. Wegscheider, T. Ihn, K. Ensslin, A. Wallraff. Phys. Rev. X, **8**, 041018 (2018). DOI: 10.1103/PhysRevX.8.041018

[11] J. Larson, T. Mavrogordatos, S. Parkins, A. Vidiella-Barranco. J. Opt. Soc. Am. B, **41** (8), JCM1 (2024). DOI: 10.1364/JOSAB.536847

[12] C.-P. Yang, Q.-P. Su, S.-B. Zheng, F. Nori. New J. Phys., **18**, 013025 (2016). DOI: 10.1088/1367-2630/18/1/013025

[13] A. Peres. Phys. Rev. Lett., **77** (8), 1413 (1996). DOI: 10.1103/PhysRevLett.77.1413

[14] R. Horodecki, M. Horodecki, P. Horodecki. Phys. Lett. A, **223**, 333 (1996). DOI: 10.1016/S0375-9601(96)00706-2

[15] W.K. Wooter. Phys. Rev. Lett., **80** (10), 2245 (1998). DOI: 10.1103/PhysRevLett.80.2245

[16] S.N. Filippov. J. Mathem. Sci., **241**, (2), 210 (2019) (in Russian). DOI: 10.1007/s10958-019-04418-3

[17] A. Barenco, Ch.H. Bennett, R. Cleve, D.P. DiVincenzo, N. Margolus, P. Shor, T. Sleator, J.A. Smolin, H. Weinfurter. Phys. Rev. A, **52**, 3457 (1995). DOI: 10.1103/PhysRevA.52.3457

[18] Y. Shi. Quant. Infor. Comput., **3**, 84 (2003). DOI: 10.26421/QIC3.1-7

[19] E. Fredkin, T. Toffoli. Int. J. Theor. Phys., **21** (3–4), 219 (1982). DOI: 10.1007/bf01857727

[20] D.G. Cory, M.D. Price, W. Maas, E. Knill, R. Laflamme, W.H. Zurek, T.F. Havel, S.S. Somaroo. Phys. Rev. Lett., **81**, 2152 (1998) DOI: 10.1103/PhysRevLett.81.2152

[21] M. Neeley, R.C. Bialczak, M. Lenander, E. Lucero, M. Mariantoni, A.D. O'Connell, D. Sank, H. Wang, M. Weides, J. Wenner, Y. Yin, T. Yamamoto, A.N. Cleland, J.M. Martinis. Nature, **467**, 570 (2010). DOI: 10.1038/nature09418

[22] L. DiCarlo, M.D. Reed, L. Sun, B.R. Johnson, J.M. Chow, J.M. Gambetta, L. Frunzio, S.M. Girvin, M.H. Devoret, R.J. Schoelkopf. Nature,**467**, 574 (2010). DOI: 10.1038/nature09416

[23] Ch.F. Roos, M. Riebe, H. Häffner, W. Hänsel, J. Benhelm, G.P.T. Lancaster, Ch. Becher, F. Schmidt-Kaler, R. Blatt. Nature, **404**, 1478 (2004). DOI: 10.1126/science.109752

[24] D.C. Cole, J.J. Wu, S.D. Erickson, P.-Y. Hou, A.C. Wilson, D. Leibfried, F. Reiter. New J. Phys., **23**, 073001 (2021). DOI: 10.1088/1367-2630/ac09c8

[25] Y. Maleki, A.M. Zheltikov. J. Opt. Soc. Am. B, **36**, 443 (2019). DOI: 10.1364/JOSAB.36.000443

[26] P. Neumann, N. Mizuochi, F. Rempp, P. Hemmer, H. Watanabe, S. Yamasaki, V. Jacques, T. Gaebel, F. Jelezko, J. Wrachtrup. Science, **323**, 1326 (2009). DOI: 10.1126/science.11572

[27] K. Takeda, A. Noiri, T. Nakajima, J. Yoneda, T. Kobayashi, S. Tarucha. Nature Nanotechnology, **16**, 965 (2021). DOI: 10.1038/s41565-021-00925-0

[28] M. Ge, L.-F. Zhu, L. Qiu. Commun. Theor. Phys., **49**, 1443 (2008), DOI: 10.1088/0253-6102/49/6/20

[29] D.-M. Lu, C.-D. Qiu. Optoelectron. Lett., **9** (2), 0157 (2013). DOI: 10.1007/s11801-013-2392-0

[30] K. Wu, Q. Huang, X. Zhang. Adv. Mater. Res., **662**, 537 (2013). DOI: 10.4028/www.scientific.net/AMR.662.537

[31] K.-I. Kim, H.-M. Li, B.-K. Zhao. Int. J. Theor. Phys., **55**, 241 (2016). DOI: 10.1007/s10773-015-2656-5

[32] W.-Ch. Qiang, G.-H. Sun, Q. Dong, O. Camacho-Nieto, Sh.-H. Dong. Quant. Information Proces., **17**, 90 (2018). DOI: 10.1007/s11128-018-1851-8

[33] D.-M. Lu. J. Mod. Opt., **66**, 424 (2019). DOI: 10.1080/09500340.2018.1537406

[34] M. Ali. Quant. Inform. Proces., **20**, 311 (2021). DOI: 10.1007/s11128-021-03195-w

[35] M. Yahyavi, M.A. Jafarizadeh, N. Karimi, A. Heshmati. Prog. Theor. Exp. Phys., **2022**, 093A01 (2022). DOI: 10.1093/ptep/ptac099

[36] C.J.-Fang, L.H.-Ping. Commun. Theor. Phys., **43**, 427 (2005). DOI: 10.1088/0253-6102/43/3/010

[37] K. Fujii, K. Higashida, R. Kato, T. Suzuki, Yu. Wada. Intern. J. Geometric Methods Mod. Phys., **01**, 721 (2004). DOI: 10.1142/S0219887804000344

[38] M. Youssef, N. Metwally, A.-S.F. Obada. J. Phys. B: At. Mol. Opt. Phys., **43**, 095501 (2010). DOI: 10.1088/0953-4075/43/9/095501

[39] J.-S. Zhang, A.-X. Chen. Intern. J. Quantum Inform., **07**, 1001 (2009). DOI: 10.1142/S0219749909005638

[40] Z.X. Man, Y.-J. Xia, N.B. An. J. Mod. Opt., **56** (8), 1022 (2009). DOI: 10.1080/09500340902887666

[41] J.-Yo. Zhou, S.-L. Zhao, Y. Yang, Sh. Xiao, D. He, W. Nie, Yi. Hu, J. Lu, L.-M. Kuang, Y.-Xi Liu, M.-T. Deng, D.-N. Zheng, Zh.-Ch. Xiang, L. Zhou, Z.H. Peng. Opt. Express, **32** (1), 179 (2024). DOI: 10.1364/OE.509250
[42] X.-W. Hou, M.-F. Wan, Z.-Q. Ma. The Europ. Phys. J. D, **66** 152, (2012). DOI: 10.1140/epjd/e2012-30018-4
[43] A.R. Bagrov, E.K. Bashkirov. Bulletin of Samara University, natural science series **28** (1–2), 95 (2022). DOI: 10.18287/2541-7525-2022-28-1-2-95-105
[44] A.R. Bagrov, E.K. Bashkirov. *IX Int. Conf. Infor. Techn. Nanotechn. (ITNT)* 1–5.
DOI: 10.1109/ITNT57377.2023.10139206
[45] L. Qiu, A.M. Wang, X.Q. Su, Opt. Commun., **281**, 4155 (2008), DOI: 10.1016/j.optcom.2008.03.078
[46] F. Han, Y.-J. Xia. Intern. J. Quantum Inform., **7**, 1337 (2009). DOI: 10.1142/S0219749909005821
[47] J.-L. Zhang, J. Ma, S.-Yu. Yu, Q. Han, B. Li. Int. J. Theor. Phys., **53**, 942 (2014). DOI: 10.1007/s10773-013-1885-8
[48] A.R. Bagrov, E.K. Bashkirov. ZhTF, **94** (3), 341 (2024) (in Russian). DOI: 10.61011/JTF.2024.03.57370.301-23
[49] R. Jozsa. J. Mod. Opt., **41**, 2315 (1994).
DOI: 10.1080/09500349414552171

Translated by T.Zorina